ICES Journal of Marine Science

ICES International Council for the Exploration of the Sea
CIEM Conseil International pour l'Exploration de la Mer

ICES Journal of Marine Science (2012), 69(4), 648–659. doi:10.1093/icesjms/fss010

Species identification in seamount fish aggregations using moored underwater video

Richard L. O'Driscoll[1]*, Peter de Joux[1], Richard Nelson[1], Gavin J. Macaulay[2], Adam J. Dunford[1], Peter M. Marriott[1], Craig Stewart[1], and Brian S. Miller[1‡]

[1]*National Institute of Water and Atmospheric Research Limited, Private Bag 14-901, Kilbirnie, Wellington 6241, New Zealand*
[2]*Institute of Marine Research, PO Box 1870 Nordnes, 5817 Bergen, Norway*

**Corresponding author: tel: +64 4 3860300; fax: +64 4 3860574; e-mail: r.odriscoll@niwa.co.nz.*
[‡]*Present address: Australian Antarctic Division, 203 Channel Highway, Kingston, Tasmania 7050 Australia.*

O'Driscoll, R. L., de Joux, P., Nelson, R., Macaulay, G. J., Dunford, A. J., Marriott, P. M., Stewart, C., and Miller, B. S. 2012. Species identification in seamount fish aggregations using moored underwater video. – ICES Journal of Marine Science, 69: 648–659.

Received 24 August 2011; accepted 4 December 2011; advance access publication 13 February 2012.

Acoustic surveys of New Zealand deep-water seamounts often show fish aggregations up to 150 m high on the summit. Although bottom trawls on the seamount slopes catch predominantly orange roughy (*Hoplostethus atlanticus*), species composition in the mid-water plumes is extremely uncertain. In June 2010, moored underwater video cameras were deployed on the summit of the Morgue seamount (summit depth 890 m), a feature that has been closed to fishing since 2001. Cameras and lights were timed to come on for 2 min every 2 h. Fish response to the mooring was monitored using vessel-mounted echosounders. Moored cameras confirmed that orange roughy were present up to 70 m above the seamount summit. Orange roughy made up 97% of the fish identified from the video. Other species observed included smooth oreo (*Pseudocyttus maculatus*), spiky oreo (*Neocyttus rhomboidalis*), deep-water dogfish, cardinalfish (*Epigonus* spp.), and squid. Total along-track backscatter from the plume varied by a factor of 25 over a period of hours. Peak acoustic densities in the plume (equivalent to 20 orange roughy m^{-3}) were an order of magnitude higher than peak visual estimates (0.64 orange roughy m^{-3}), but relative densities between paired video and acoustic observations were generally consistent.

Keywords: acoustics, mark identification, orange roughy, seamounts.

Introduction

Seamounts are important features of the New Zealand marine environment. There are ~800 features with vertical elevation >100 m above the surrounding seafloor known from the general New Zealand region (Rowden *et al.*, 2005). Major fisheries for orange roughy (*Hoplostethus atlanticus*), oreos (black oreo *Allocyttus niger* and smooth oreo *Pseudocyttus maculatus*), black cardinalfish (*Epigonus telescopus*), alfonsino (*Beryx splendens*), bluenose (*Hyperoglyphe antarctica*), and rubyfish (*Plagiogeneion rubiginosum*) occur on and around New Zealand seamounts (Clark and O'Driscoll, 2003; O'Driscoll and Clark, 2005). In the mid 1990s, 60–70% of the New Zealand orange roughy catch was taken from seamounts (Clark and O'Driscoll, 2003), although this proportion has subsequently decreased to less than 50% (NIWA, unpublished data). Seamount fisheries also occur in many other regions, prominently in the Pacific Ocean, but also in the southern Indian Ocean, the mid-Atlantic Ridge in the North Atlantic, and off the African coast in the south Atlantic (review by Clark, 2009).

Acoustic surveys of deep-water seamounts often show fish aggregations (commonly described as "plumes") up to 150 m high on the summit (e.g. Bull *et al.*, 2001). Species composition in these aggregations is extremely uncertain. Although demersal trawls on the seamount slopes catch predominantly orange roughy, attempts to sample the midwater plumes using nets and towed and lowered cameras have been unsuccessful due to fish avoidance (Koslow *et al.*, 1995; Kloser *et al.*, 1996, 2002). Due to the low target strength (TS) of orange roughy relative to associated species (McClatchie and Coombs, 2005a), species composition is a major source of uncertainty in interpreting acoustic survey results from seamounts (Kloser *et al.*, 2002; Doonan *et al.*, 2009). Acoustic discrimination of species using towed multifrequency acoustics shows some promise for deep-water species (e.g. Kloser *et al.*,

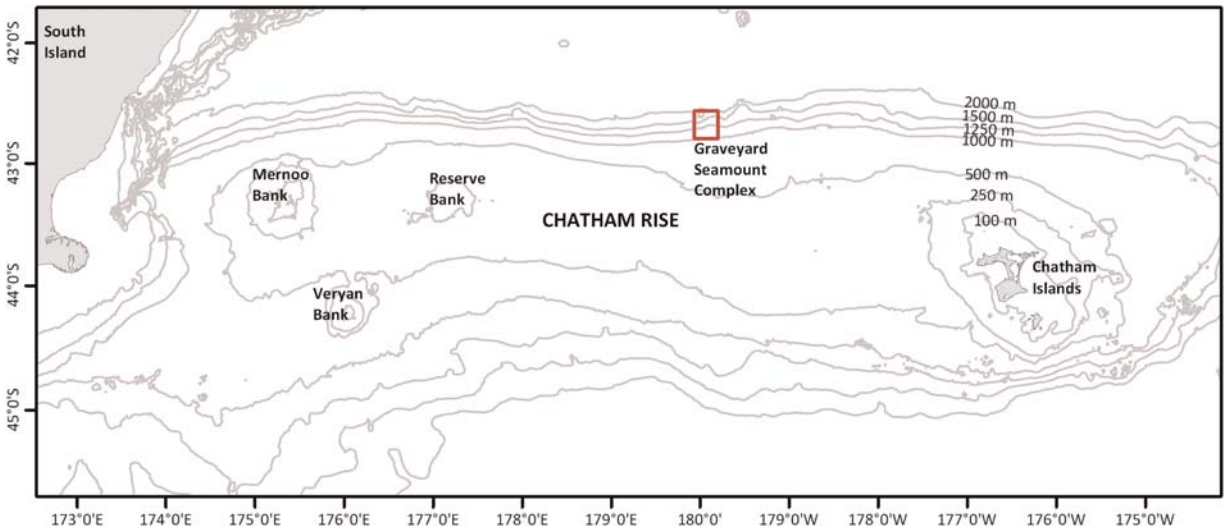

Figure 1. Location of Graveyard seamount complex on the north Chatham Rise, east of New Zealand.

2002), but this method still requires independent (i.e. non-acoustic) verification (or "ground-truthing").

Our aim was to develop a tool for directly evaluating species composition in undisturbed deep-water acoustic marks (throughout this paper, the colloquial term "mark" is used to describe the acoustic backscatter associated with an aggregation of fish). An attempt to moor video cameras in aggregations in 2007 showed promise. The cameras used on these trials suffered from technical problems which resulted in little useful video footage. However, vessel-mounted acoustic observations of the reaction of the aggregations to the mooring were informative, apparently showing that the aggregations became accustomed to the mooring and approach to within the range of video cameras. This paper describes results from our experiments with moored cameras in June 2010.

Methods

Study location

Three moorings were deployed on Morgue seamount (summit depth 890 m) on the north Chatham Rise, east of New Zealand (Figure 1). This feature was chosen for our study as it has a relatively dense and predictable acoustic mark on its summit and it has been closed to all trawling since May 2001. Morgue is part of the Graveyard seamount complex, which includes both fished and unfished features (McClatchie and Coombs, 2005b; Clark *et al.*, 2010). An estimated cumulative catch of 8769 t of orange roughy has been taken from the Graveyard seamounts from 1980 to 2009 (Ministry of Fisheries, 2010).

Mooring design and deployment

Each mooring comprised: 1–3 video cameras and lights looking horizontally, 1–3 RCM9 current meters next to each camera, a Seabird Microcat SBE-37 salinity and temperature data logger, an anchor weight, two acoustic releases in a redundancy system to attach the mooring to the anchor weight, floats to provide buoyancy, and a Sabel radio-locating beacon. A summary of each mooring configuration is provided in Table 1. The total height of the mooring was 70–120 m above the seafloor. The number and spacing of cameras was determined by the gear available and the vertical distribution of the mark above the seamount. Moorings were positioned as close as possible to the summit of the seamount, which is where the acoustic mark was usually observed.

The mooring was assembled as it was lowered over the side of the vessel, anchor weight first. An acoustic release and acoustic positioning device transponder (Simrad HPR) was attached to the top of the mooring after the entire mooring was hanging in the water and a cable was connected to the top acoustic release. The whole assembly was then lowered so that the anchor weight was ~40 m above the seafloor. Real-time positions of the top of the mooring were obtained from the HPR so that the top of the mooring could be precisely positioned over the deployment location. The top acoustic release was then activated, allowing the mooring to fall the final few metres to the seafloor. The mooring was sometimes visible on the vessel's echosounders and this provided a check that it was deployed correctly. To retrieve the mooring, one of the lower acoustic releases was activated. The anchor weight (200 kg iron wheel) remained on the seafloor and had ceramic tiles cemented to it that will subsequently act as a settlement site for benthic organisms, to be revisited on future voyages.

The video cameras used on the mooring were 3.6 Megapixel Sony XR200VE digital handycams mounted inside a custom-made cast 2205 stainless steel housing with 20 mm thick acrylic viewports. The camera angle of view was 43° in air, which was estimated theoretically to be equivalent to 32° in water once refraction of the acrylic housing viewport and seawater were taken into account. The theoretical field of view was checked in a tank and was found to be close to the empirical estimate. Digital video data with a 16:9 aspect ratio were recorded in AVCHD format to the camera's internal 120 GB hard drive. Lighting was provided by custom-built LED lights. Each light was constructed by encapsulating two 5 W LED MR16 downlight bulbs within a block of clear acrylic resin. Each LED downlight bulb had a 30° viewing angle with an intensity of 300 lumens at the "cool white" colour temperature of 5100 K. The video camera and lights were controlled using a custom-built microprocessor that communicated with the video camera via the Sony LANC protocol into a command and control port on the

Table 1. Summary of mooring deployments.

Mooring	Latitude	Longitude	Deployment time (NZST)	Release time (NZST)	Number of cameras	Estimated camera heights above seabed (m)	Measured camera depths (m)	Camera timing	Number of acoustic transects	
									East–west	North–south
1	42°43.00′S	179°57.55′W	17 June 11:39	18 June 07:30	3	10, 50, 100	818, 863, 910	6 min every 10 min from 15:00[a]	11	7
2	42°43.01′S	179°57.58′W	24 June 13:00	25 June 08:33	1	50	853	2 min every 2 h	18	2
3	42°43.01′S	179°57.58′W	27 June 08:50	29 June 08:48	2	30, 70	832, 878	2 min every 2 h	29	4

[a]Programming error.

camera. The camera, lights, and microprocessor were powered by a 14.4-V lithium ion rechargeable battery pack of 15 Ah capacity, also located within the stainless steel housing. The camera housing and two sets of lights (0.5 m above and below the camera housing) were bolted to a stainless steel frame that was then clamped to the mooring line. The orientation of the cameras for all deployments was horizontal, but no attempt was made to keep them pointed in any particular compass direction. Depth sensors in the adjacent RCM9 current meters provided accurate estimates of the depth of each camera during the deployments (Table 1).

Cameras and lights were remotely programmed to turn on and off at intervals (Table 1) with the camera starting recording 10 s before the lights came on. In the first deployment, cameras were supposed to be set to turn on for 5 min every hour from 15:00 NZST (i.e. a delay of 3 h 21 min after the mooring was deployed at 11:39 NZST to the first recording). However, due to a programming error, they were actually set to turn on for 6 min every 10 min from 15:00. This error was identified overnight and the mooring was retrieved at daylight (07:30 NZST) on 18 June. In the second and third deployments, cameras were timed to come on for 2 min every 2 h (i.e. at 00:00, 02:00, 04:00, etc.) with no time delay before the first recording.

Acoustics

Acoustic transects were run over the deployment sites to provide information on the distribution of aggregations around the seamount and to monitor their behavioural response to the mooring and light bursts. Multifrequency acoustic data (at 18, 38, 70, 120, and 200 kHz) were collected from the vessel-mounted Simrad EK60 echosounders on RV "Tangaroa" but, because of the water depth, only data from 18 and 38 kHz echosounders were suitable for analysis. Echosounders were calibrated on 27 January 2010 using a 38.1-mm tungsten carbide sphere following the standard scientific protocols (Simmonds and MacLennan, 2005). The seawater propagation parameters of absorption and sound velocity were calculated from the formulae of Doonan *et al.* (2003) and Fofonoff and Millard (1983), respectively, based on temperature and salinity profiles obtained with the Microcat SBE37 CTD as the mooring was sinking.

In all, 71 acoustic transects were made during the three deployments (Table 1). Most (58) of these transects were orientated east–west. This transect orientation gave the best data quality in both directions (i.e. east–west and west–east) under the prevailing weather conditions. Several attempts were made to hold the vessel stationary over the mooring position as the camera and lights came on, but these were unsuccessful as we were not able to maintain vessel position to the required accuracy.

Video analysis

The software ACDSee Pro3 was used to view the video and generate screen grabs. All organisms in the video were identified to the finest resolution possible and fish behaviour was described. Quantitative analysis was based on still images (frame grabs) selected at 10 s intervals from the recording. The first selected image was the frame when the lights first went on, which we regarded as the best measure of undisturbed fish density and orientation.

Image analysis was carried out using Image-J software. In all selected images, organisms were identified and counted, along

with qualitative estimates of range and quality. The optical description of those range bins is as follows:

Very close: Fish brightly illuminated and would fill a significant portion of the frame if centred in it.

Close: Fish well illuminated and fish colour is obvious. Fish outlines well defined.

Mid: Fish poorly illuminated, colour washed out. Fish outlines are a little hazy.

Distant: Fish faintly illuminated, no colour. Fish outlines poorly resolved and resolution often too poor for behavioural observations and measurements.

The approximate ranges corresponding to each of the four bins were estimated from the relationship of the frame size dimensions in pixel counts to the length of side-on view fish observed in pixels, assuming that all orange roughy were ~34 cm standard length (*SL*). Because Morgue is closed to fishing, we do not have estimates of the size of orange roughy on this feature in 2010. Commercial catches from the adjacent Graveyard seamount in the same period (26–30 June 2010) had mean *SL* of 33.8 cm for orange roughy (I. Hampton *et al.*, pers. comm.). The mean length of orange roughy in five research trawls on Morgue from 22 June to 6 July 1999 was 32.9 cm *SL* (Bull *et al.*, 2000).

Measurements of fish fork length (*FL*; in pixels) and orientation were made for fish that appeared to be side-on to the camera. *FL* was measured because this was easier to estimate from the images. A regression converting *FL* to *SL* for orange roughy was estimated using the empirically derived relationship $SL = 0.8805\,FL$ ($n = 321$, $r^2 = 0.998$), which was obtained from the subset of images where both measurements were possible.

Acoustic analysis

Acoustic data were visualized and analysed using Echoview®. Initial processing was carried out to define the seafloor and edit out noise caused by bubble aeration and missing transmits. Particular care was taken to exclude side-lobe echoes caused by the steeply sloping seafloor. In general, acoustic data quality was very good due to relatively calm weather and sea conditions during the periods when the moorings were deployed. Echogram regions were drawn manually to outline the seamount plume. In all instances, the aggregation was relatively well-defined. Acoustic data were integrated at both 18 and 38 kHz in cells corresponding to 100 m along-transect by 5 m depth. This cell size was chosen as approximating the finest resolution appropriate for the acoustic data, given a theoretical beam diameter for the 38-kHz transducer (nominal 7° beam width between −3 dB points) of 100 m at 800 m range. The estimated sampling volume contained within each acoustic cell was therefore ~50 000 m^3 (100 m by 100 m by 5 m) at the depth of the mark.

Data were summarized as the mean volume backscattering strength for each cell (S_v in dB and its linear equivalent s_v in $m^2\ m^{-3}$; MacLennan *et al.*, 2002). Estimates of total along-track backscatter from the aggregation (in $m^2\ m^{-1}$) were obtained by summing the proportioned region to cell area mean backscattering coefficients (in $m^2\ m^{-2}$ = PRC_ABC in Echoview) for each cell along the transect and multiplying by the cell length (100 m). This metric is equivalent to multiplying the mean areal backscattering coefficient (s_a) for the transect by the transect length (in m).

Estimates of s_v were converted to acoustic estimates of equivalent orange roughy density (in fish m^{-3}) using the estimated acoustic TS for orange roughy of −52.1 dB. This estimated TS was derived from *in situ* estimates of visually verified orange roughy targets with mean *SL* of 33.9 cm (NIWA and CSIRO, unpublished data).

To compare acoustic density estimates with video estimates of fish density, we selected the cell on the echogram which corresponded to the measured depth and estimated location of the camera. The mooring was not acoustically visible within the cell when the aggregation surrounded the mooring. Because there was often some uncertainty about the exact location of the mooring, we also looked at the grid of eight cells next to the "mooring cell". Minimum and maximum estimates of acoustic density around the camera were calculated from the minimum and maximum s_v in these nine cells.

The s_v of the camera and mooring floats was empirically estimated from transects where the aggregation was not present around the mooring (mainly in the first deployment). The mean estimated S_v for the mooring was −67.6 dB (equivalent $s_v = 1.74 \times 10^{-7}\ m^2\ m^{-3}$) and this contribution was subtracted from the mooring cell when estimating orange roughy density. However, because the mooring is a point source and its position in the beam is variable, this estimate was uncertain (range of measured mooring S_v −65.7 to −70.2 dB).

Results

Unfortunately, all three of the camera housings leaked during the first deployment on 17 June. Video data from two of the cameras (at 818 and 910 m) was unrecoverable and it is unknown when these cameras and lights failed. The lights of the third camera (at 863 m) and timing microprocessor were still working when the mooring was retrieved, but sufficient water had entered the housing to cause the camera to fail. Eleven 6-min long video files were recovered spanning 110 min. Analyses of these 11 clips showed few fish.

After a period of bad weather, the second mooring was deployed on 24 June. This mooring had only one camera, at ~50 m above the seafloor. This camera placement was chosen based on our acoustic observations of the mark before deployment, which suggested that the mark was relatively dense but only ~60 m high. The mooring was retrieved after ~19 h. The period of deployment was shorter than planned, but further rough weather was forecast and we wanted to check the performance of the camera. The camera and lighting performed flawlessly, and ten 2-min long video files were collected while the mooring was in place. All the video clips showed fish, with some excellent recordings of orange roughy, as well as smooth oreo, and deepwater sharks (e.g. Figure 2).

The third and final mooring was deployed on 27 June. This mooring had two cameras, at ~30 and 70 m above the seafloor. This camera placement was chosen to bracket the observations from 50 m during mooring 2. The mooring was retrieved after ~48 h. Both cameras and lighting turned on as scheduled every 2 h, resulting in 24 2-min long video files were collected from each camera while the mooring was in place. High-quality recordings of orange roughy and other species were recorded from both cameras (e.g. Figure 2).

Figure 2. Selection of screen-grabs from the video during second and third mooring deployments. Clockwise from top left: orange roughy at 853 m depth on 25 June; school of orange roughy at 853 m on 24 June; school of orange roughy at 878 m on 27 June; deep-water dogfish (probably *Centroscymnus owstoni*) at 853 m on 25 June; smooth oreo with orange roughy in background at 853 m on 24 June; orange roughy at 832 m on 29 June.

Oceanographic context

Mean temperature and salinity at 880-m depth were 6.2°C and 34.4 psu, respectively. Current meters indicated a periodic north–south current, with a net westward flow. Mean current speeds were between 6.2 and 16.5 cm s^{-1}, with highest observed mean current close to the seamount summit (910 m water depth) during mooring 1 and lowest mean current speed at 853 m during mooring 2.

Video analysis

A summary of species observed on the video is given in Table 2. Orange roughy made up 97% of the species counted from selected frames. Other species identified included smooth oreo (*P. maculatus*), spiky oreo (*Neocyttus rhomboidalis*), deep-water dogfish (several species probably including *Centroscymnus owstoni*, *Etmopterus baxteri*, and *Dalatias licha*, which could not be reliably discriminated), cardinalfish (*Epigonus* spp.), and squid (species unknown). Small gelatinous zooplankton (possibly jellyfish or salps) were also commonly observed but could not be easily quantified. The number and species composition of fish varied considerably between each video clip. Only three fish were recorded during the first mooring deployment, when lights were on for 6 min every 10 min. In the second deployment, orange roughy were observed in nine of ten video clips from the camera at 853 m (Table 2). In the third deployment, orange roughy were present in 23 of the 24 clips from 878 m, but only 12 of 24 clips from 832 m (Table 2). Fish counts at 832 m were also usually lower than those observed during the same deployment at 878 m (Table 2). Although there was weak evidence of a diel pattern in orange roughy counts during the third mooring, with highest counts observed between 02:00 and 14:00 NZST, the duration of the mooring was not long enough to determine whether this was a consistent pattern.

The number of fish counted in each of the four qualitative range bins is given in Figure 3. Figure 3 also shows the maximum ranges of measured orange roughy in each range bin. Ranges are maximal because they assume that all fish were perfectly side-on to the camera (90° incidence). If incidence angles were greater than or less than 90° then the range to the fish will be

Table 2. Species observed on the video during mooring deployments.

	Mooring 1 (863 m)			Mooring 2 (853 m)			Mooring 3 (832 m)			Mooring 3 (878 m)		
Common name	Clips ($N = 11$)	Frames ($n = 396$)	Count	Clips ($N = 10$)	Frames ($n = 120$)	Count	Clips ($N = 24$)	Frames ($n = 288$)	Count	Clips ($N = 24$)	Frames ($n = 288$)	Count
Orange roughy	1	1	1	9	88	522	12	93	322	23	252	2739
Smooth oreo	1	1	1	2	2	2	0	0	0	9	16	19
Spiky oreo	0	0	0	2	4	4	1	1	1	3	4	4
Deep-water dogfish	1	1	1	6	18	22	9	21	21	6	22	31
Cardinalfish	0	0	0	0	0	0	0	0	0	2	2	2
Squid	0	0	0	0	0	0	1	1	1	0	0	0
Unidentified fish	0	0	0	0	0	0	0	0	0	1	0	1

Clips, the number of video clips when the species was present; Frames, the number of selected frames (grabbed every 10 s) when the species was visible; Count, the summed total number of the species observed in selected frames; *N*, the number of video clips; *n*, the number of frames selected from each camera.

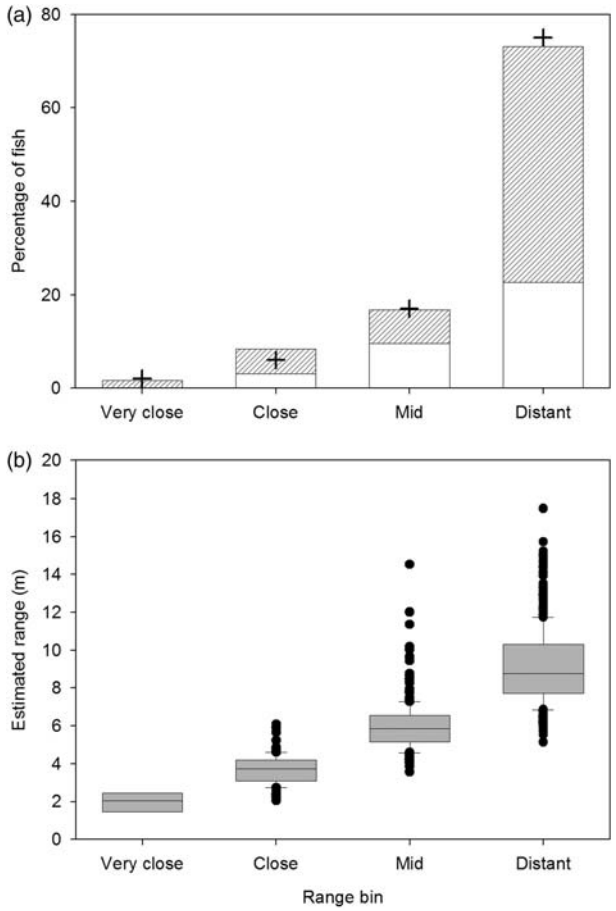

Figure 3. (a) Percentage of fish in each of four qualitative range bins; and (b) estimated maximum range to measured orange roughy in each bin from all analysed frames. In (a), white portions of each bar show the proportion of fish that could be measured and shaded portion are fish which were not measured. Crosses show the expected proportion of targets in each range bin based on sampling volume if fish are of uniform density and range bins have the following limits: very close, <3 m; close, 3–5 m; mid, 5–7 m; distant 7–10 m. In (b), ranges were estimated assuming that all orange roughy were 34 cm *SL* and were side-on (90° incidence) to camera. Boxes are the 25th and 75th percentiles divided by the median, whiskers show the 5th and 95th percentiles, and outliers are shown as solid circles.

overestimated. For example, a 34-cm orange roughy quartering away from the camera (45° incidence) at 6 m range would be estimated as being at 8.4 m. Conversely, the selection of targets that could be measured was also biased at short and long ranges (Figure 3). At close ranges, most visible fish were only partially in the frame. At distant ranges, a large proportion of fish were too indistinct to accurately resolve the outline and make measurements.

Our best estimates of the ranges corresponding to each of the four qualitative bins were based on the 25th and 75th percentiles of the maximum range to measured orange roughy (Figure 3). These were: very close, <3 m; close, 3–5 m; mid, 5–7 m; and distant, 7–10 m. Using these range limits, the number of observed fish in each bin was very similar to the expected number based on the relative sampling volume, assuming that fish density was independent of range (Figure 3). Our best estimate of the detection range of camera and lights was 10 m, which gave a sampling volume of 61 m^3. Video estimates of fish density (fish m^{-3}) were also calculated based on detection ranges of 8 and 12 m (equivalent to sampling volumes of 31 and 105 m^3, respectively).

Using the best estimate of camera detection range of 10 m, the peak frame count of 39 orange roughy from the camera at 878 m at 14:00 on 27 June corresponds to a density of 0.64 fish m^{-3}. Peak orange roughy density estimates based on the minimum and maximum estimated detected ranges of 8 and 12 m were 1.26 and 0.37 fish m^{-3} respectively. Corresponding estimates of peak densities for smooth oreo and deep-water dogfish were four oreos and three dogfish per frame which was equivalent to 0.066 and 0.049 fish m^{-3} respectively, using the best estimate of sampling volume.

Qualitative behavioural observations showed orange roughy drifting, remaining stationary, burst swimming, occasionally feeding, and even colliding with the camera. On several occasions, orange roughy appeared to be stunned by the lights and froze when close to the camera (e.g. top right panel in Figure 2). At the start of the recordings, immediately after the lights were turned on, orange roughy were usually orientated in the same direction and with heads tilted slightly down (Figure 4). Most fish were moving very slowly. Vertical tilt-angles were estimated from 1273 orange roughy, which were approximately broadside to the camera. There was a broad range of tilt-angles observed, but a clear increase

in median tilt-angle with increasing time after the camera lights turned on, consistent with diving behaviour (Figure 4). This pattern was observed from all three camera depths.

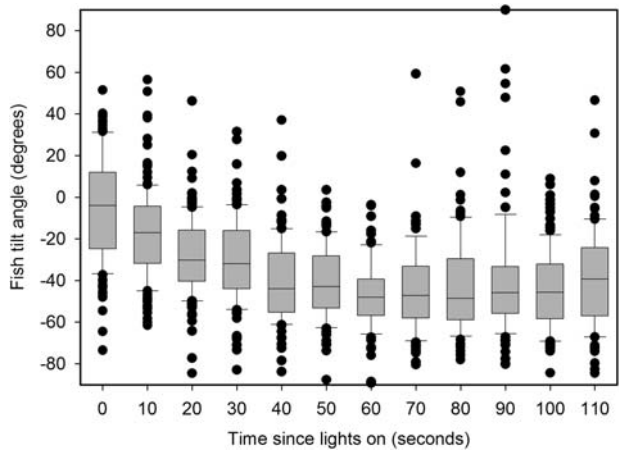

Figure 4. Change in tilt-angle of measured orange roughy with increasing time after lights turned on. Data from all three cameras on moorings 2 and 3 are combined. Negative tilt-angle indicates that fish are head-down. Boxes are the 25th and 75th percentiles divided by the median, whiskers show the 5th and 95th percentiles, and outliers are shown as solid circles.

Acoustic analysis

There were 18 acoustic transects over the mooring during the first deployment (Table 1). The acoustic mark before deploying the first mooring was ~120 m high (Figure 5a). This mark was still in a similar location after the mooring was deployed but before the lights were turned on (Figure 5b and c). As soon as the lights turned on at 15:00, a response was detected acoustically where the mark divided around the mooring (Figure 5d). The layers immediately above the mooring also became much less dense, leaving a lighter "halo" which was obvious in the echograms (Figure 5e–k). This avoidance behaviour was still apparent until the mooring was retrieved, although there was some evidence that the main mark was re-grouping around the mooring in the last two passes as 06:00 and 06:31 on 18 June (Figure 5j and k). The strong avoidance response was probably a result of the programming error which meant that the lights were on virtually continuously.

There were 20 transects over the mooring during the second deployment and 33 transects during the third deployment (Table 1). Many of these transects were timed to pass over the mooring immediately before and/or after the periods of filming to monitor the reaction of the acoustic mark to the lights (e.g. Figure 6a–d). Our acoustic observations suggested that there was a discernible response to the lights (usually the mark reduced in height or sometimes split at a depth equivalent to the height of the camera), but this response was of relatively short duration, and the acoustic mark reformed within 30 min (Figure 6d).

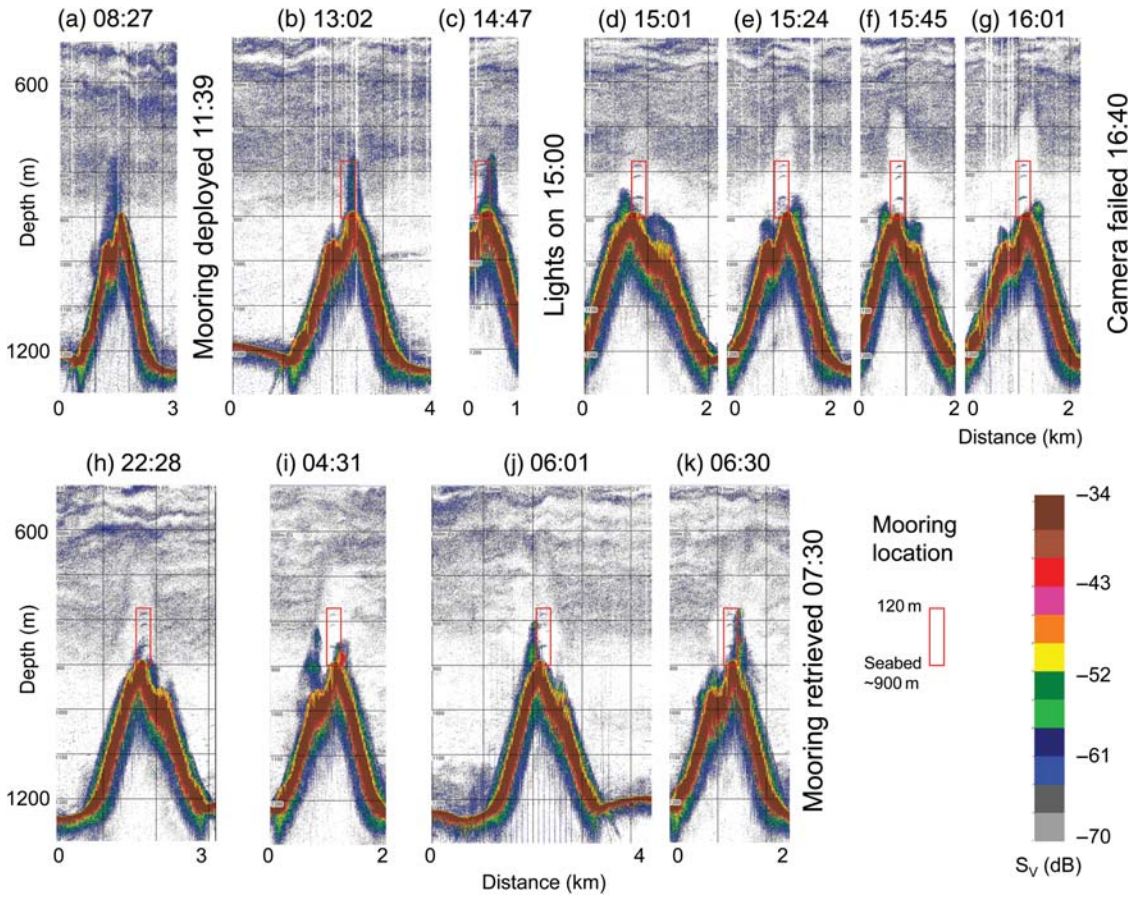

Figure 5. Montage of 38-kHz acoustic echograms collected during the first mooring deployment on Morgue 17 and 18 June. Echograms have been manipulated so all transects are orientated west to east.

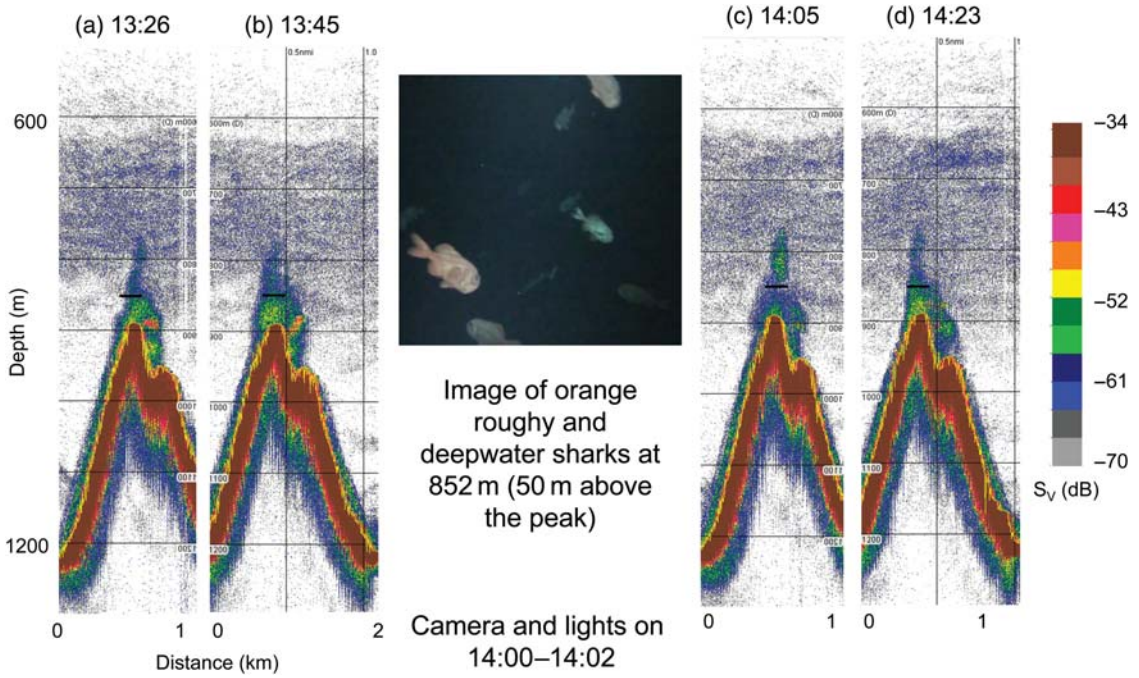

Figure 6. Montage of 38-kHz acoustic echograms showing typical response to lights during second mooring deployment on 24 June 2010. Horizontal bar in echograms shows the approximate location of the camera and lights. Echograms have been manipulated so all transects are orientated west to east.

There were eight occasions during moorings 2 and 3 where we had paired transects with the same orientation (east–west) <30 min before and <30 min after the lights came on. Acoustic data from these paired transects were used to test whether there were consistent changes in the structure of the aggregation in response to the lights. Four variables were considered: total along-track backscatter from the mark, mean weighted mark depth, mean weighted mark position (longitude), and mean volume backscattering strength (S_v) in the cell(s) surrounding the camera(s). Mean aggregation depth increased in 6 of 8 occasions (diving), the aggregation moved further east in 7 of 8 occasions (displacement), and acoustic density around the camera decreased after the lights went on in 8 of 13 observations, but none of these changes were statistically significant (paired sample *t*-test, $p > 0.05$) due to the small sample size. There was no consistent change in total along-track backscatter in response to the lights.

There was also considerable short-term variability in the density and structure of the acoustic mark which did not seem to be related to the presence of the mooring. Figure 7 compares total along-track backscatter from the aggregation on Morgue over the course of the second and third mooring deployments. Total backscatter varied by a factor of 25. On several occasions, there was a rapid change in total backscatter between consecutive transects over the aggregation. We have termed these "plume peak" events. Plume peak events were characterized by high S_v (greater than −50 dB) in many cells at both 18 and 38 kHz.

Comparison of video and acoustic estimates of fish density

Visual estimates of orange roughy density from the first selected frame after the lights turned on every 2 h ranged from 0 to 0.64 fish m^{-3} with a mean estimate (unweighted) from all three cameras of 0.12 fish m^{-3}. As noted previously, observed orange roughy density increased with increasing depth, with mean visual density estimates from cameras at 833, 852, and 878 m of 0.02, 0.10, and 0.23 fish m^{-3}, respectively. Corresponding acoustic estimates, assuming all backscattering in the cell surrounding the camera was from orange roughy with mean TS of −52.1 dB, ranged from the equivalent of 0.004–14.6 orange roughy m^{-3}. Two very high acoustic estimates (equivalent to densities >10 fish m^{-3}) were recorded. These corresponded to cells within plume peak events. When these two high values were removed, mean acoustic density estimates from cells surrounding cameras at 833, 852, and 878 m of 0.07, 0.37, and 0.98 fish m^{-3}, respectively. Therefore, mean estimates of orange roughy density from acoustics were higher than video estimates but relative densities between observations were generally consistent when the infrequent plume peak events were removed.

Because acoustic estimates were from transects over the seamount, and cameras were coming on for only 2 min every 2 h, it was difficult to temporally match density observations. To further investigate the correlation between acoustic and visual estimates, we restricted our analysis to the eight acoustic transects that were <30 min before the camera and lights went on. These transects provided the best acoustic representation of the undisturbed aggregation. These eight transects gave 13 point estimates of acoustic density from the cells corresponding to the camera (three at 852 m from mooring 2 and five at each of 833 and 878 m from mooring 3) to correlate with visual estimates of density from the first frame of the subsequent video clip (Figure 8).

There was no significant correlation between the 13 paired observations (Pearson's correlation coefficient, $r = -0.13$, $p = 0.65$). However, the highest acoustic observation of 10.5 fish m^{-3} occurred within a plume peak event. The best estimate of the camera position suggested that the camera was

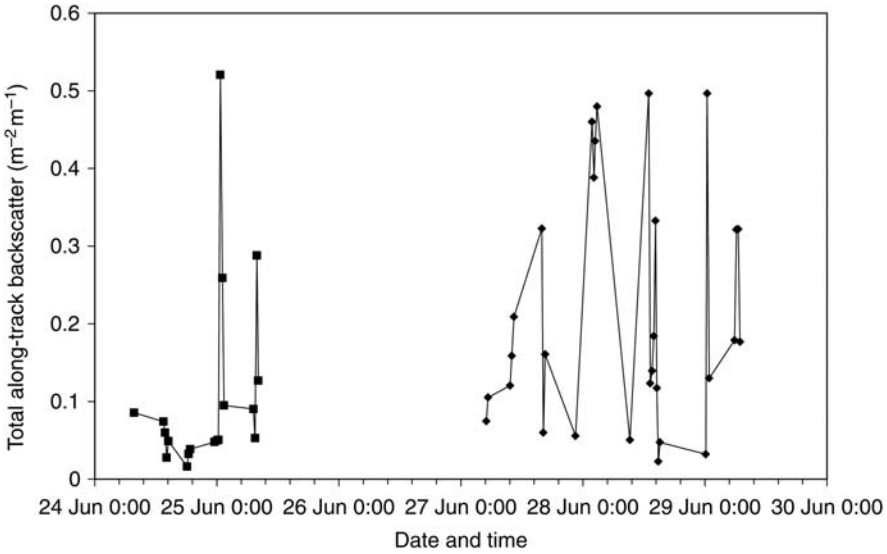

Figure 7. Changes in total along-track backscatter (at 38 kHz) from the aggregation recorded on transects with east–west orientation during the second and the third mooring deployments on Morgue. Short duration plume peak events (see text for details) are shown.

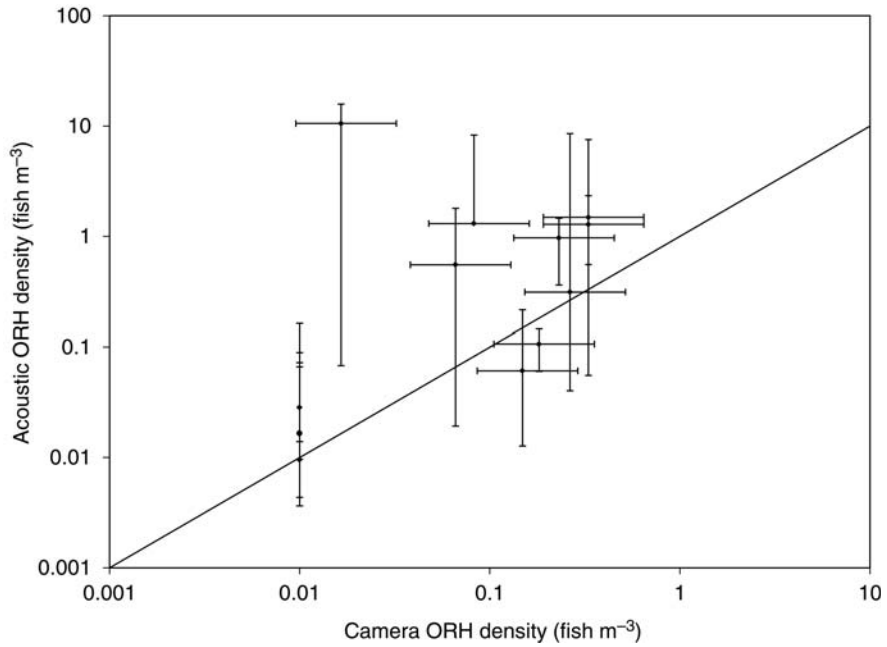

Figure 8. Comparison of estimated orange roughy (ORH) density from paired acoustic and video observations. Note log-scale on both axes. The detection threshold for the video was 0.02 fish m^{-3} (one fish visible in selected frame): frames where no orange roughy were observed on the video were plotted as 0.01 fish m^{-3}. Points show best estimates of density. Error bars on *x*-axis are based on the observed minimum and maximum camera sampling volumes. Error bars on *y*-axis are based on the minimum and maximum observed S_v from the cluster of nine acoustic cells surrounding the camera. Line shows 1:1 relationship.

within one of the acoustic cells with high density, but there was considerable uncertainty as acoustic densities in several of the surrounding cells were much lower (Figure 8). If this point was ignored, there was a significant positive correlation between the remaining 12 points ($r = 0.66$, $p = 0.02$). The slope of the best-fit (linear) regression of these 12 points was 3.42, i.e. acoustic estimates of orange roughy density were more than three times higher on average than visual density estimates.

Figure 8was based on unpartitioned acoustic backscatter (i.e. assuming all backscatter was from orange roughy). Of the 13 paired observations plotted in Figure 8, only two of the camera frames contained fish other than orange roughy (one frame showed a smooth oreo and one frame showed two deep-water dogfish). When the acoustic backscatter was partitioned to take account of these other species (using an estimated TS of −44.4 dB for smooth oreo and −38.9 dB for deep-water

dogfish), the correlation (again excluding the point from the plume peak event) decreased slightly, but was still statistically significant ($r = 0.61$, $p = 0.03$) and the slope of the best-fit regression declined to 3.15.

Discussion

Moored video cameras successfully allowed us to record species composition in midwater aggregations on seamounts. The aggregation on Morgue showed a clear avoidance response to light in the first deployment when, in error, lights were on most of the time (Figure 5). In subsequent deployments, lights and cameras were timed to come on for only 2 min every 2 h. Fish response to the lights was observed visually and acoustically: median fish tilt-angle increased as orange roughy dived (Figure 4) and aggregation acoustic characteristics changed. However, these responses appeared to be short-lived with the aggregation typically reforming within 30 min (e.g. Figure 6). The habituation time may vary between seamounts. In our previous trials in 2007, we noted that while marks on Morgue surrounded their mooring within 1.5 h after deployment, the aggregation on another feature (Cameron seamount on the Northeast Chatham Rise) only came within 40 m of the mooring after 13 h. Fish avoidance behaviour may be reduced by using red or infrared lighting (e.g. Widder *et al.*, 2005). We considered using red lighting for this study but rejected this because of the requirement for specialized low-light cameras to compensate for the increased attenuation loss at longer wavelengths.

Fish were observed close to the camera when the lights first turned on. Therefore, the first frames of each video recording appear to provide snapshots of fish density and species composition in undisturbed aggregations. However, no sampling method is unbiased and different species may exhibit different spatial and temporal behaviours in response to the mooring. For example, pelagic species are well known to aggregate around structure, and moored fish aggregation devices are used throughout the world to concentrate fish for capture (review by Dempster and Taquet, 2004). Demersal fish may also be attracted to moored and anchored structures (e.g. Wilhelmsson *et al.*, 2006). Another potential sampling bias would occur if species contributing to acoustic backscatter are too small to resolve on the video (e.g. zooplankton). The theoretical pixel resolution of our video system was ~2 mm at 6 m range, but our ability to detect targets was influenced by the lighting and contrast and was probably closer to 10 mm at 6 m. At times, we observed many small gelatinous organisms (probably salps), which appeared to be drifting passively with the current and which were impossible to accurately enumerate. Despite these potential biases, moored cameras were more successful and less intrusive than previous ground-truthing methodologies attempted on seamounts such as towed or drifting cameras and trawling (Koslow *et al.*, 1995; Kloser *et al.*, 1996, 2002).

The major disadvantage in using the moored video to ground-truth acoustic marks in that the visual range and sampling volume of the cameras are very low relative to the acoustics sampling volume: in this study, ~60 m^3 for the camera compared with 50 000 m^3 for acoustics. The temporal coverage of the camera is also very short, with our optical analysis based on only one frame every 2 h, whereas acoustic data are collected over several minutes on each transect over the seamount. Consequently, cameras provide only a glimpse at a small piece of what is contributing to backscatter. Using camera, observations to draw conclusions about mark composition, especially if this is then used to partition backscatter (e.g. O'Driscoll, 2003; McClatchie and Coombs, 2005a), require us to extrapolate that species density and composition are relatively homogeneous at scales 3 orders of magnitude larger than those observed. Visual observations are therefore not particularly suitable for detecting rare or patchy species and events. It is notable that correlation between acoustic and camera observations was improved when the very high acoustic density observed in a plume peak event was ignored (Figure 8). The use of moored cameras also requires the aggregation of interest to occur in a predictable location. This is the case for seamounts, where aggregations are strongly and consistently associated with the summit (e.g. Bull *et al.*, 2001; McClatchie and Coombs, 2005b).

Video observations showed a large proportion of orange roughy, which appears to confirm trawl catches from seamount slopes. There has been no trawling on Morgue, since it was closed to fishing in May 2001, but five trawls on this seamount as part of a research survey from 22 June to 6 July 1999 had a combined catch of 20 391 kg, of which 72% was orange roughy, 8% smooth oreo, and 20% Baxter's lantern dogfish (Bull *et al.*, 2001). In 2010, commercial trawl catches from the adjacent Graveyard seamount contained 98.3% orange roughy by weight, with a mean catch of 13.1 t per tow (I. Hampton, pers. comm.). Tracey *et al.* (2004) reported that orange roughy dominated catch rates in research trawls on the Northwest Chatham Rise, with the next nine most abundant species being five species of deep-water dogfish (*E. baxteri*, *Centroscymnus plunketi*, *D. licha*, *Deania calcea*, and *Centrophorus squamosus*), smooth oreo, black oreo (*A. niger*), black cardinalfish (*E. telescopus*), basketwork eel (*Diastobranchus capensis*), and warty squid (*Moroteuthis* spp.).

Although orange roughy dominated video observations from Morgue, estimated acoustic densities were usually higher than the observed video densities of orange roughy (Figure 8). Other species may contribute a significant proportion of the backscatter, even when the densities are much lower than the density of orange roughy, because of relatively low TS of orange roughy (McClatchie and Coombs, 2005a). For example, the overall species composition from the video frames for all cameras showed 97.0% orange roughy (by number), 2.0% deep-water dogfish, 0.8% smooth and spiky oreos, and 0.1% other swimbladder fish (Table 2). When the acoustic backscatter was partitioned to take account of these other species (using TS of −52.1 dB for 33.9 cm *SL* orange roughy, −44.4 dB for 31 cm total length smooth oreo, −38.9 dB for 80 cm total length deep-water dogfish, and −33.2 dB for 35 cm *FL* black cardinalfish), only 64% of the total backscatter is estimated as being from orange roughy.

A striking observation from this study was that total along-track acoustic backscatter from the seamount aggregation could vary by an order of magnitude between consecutive transects. At a much smaller scale, the density of fish from the same moored camera also varied considerably between video clips 2 h apart. The occurrence of considerable short-term variability within the seamount aggregation differed from the findings of Bull *et al.* (2001), who concluded that the orange roughy aggregation on the neighbouring Graveyard seamount was relatively stable over a 4-d period.

Volume backscattering strength estimates of up to −39 dB were observed within plume peak events. This is equivalent to orange roughy densities of 20 fish m^{-3}, much higher than peak visual estimates of 0.64 orange roughy m^{-3}. Using the estimates

of TS above, equivalent densities of smooth oreo, deep-water dogfish, or black cardinalfish required to produce such high acoustic backscatter are 3.5, 1.0, and 0.3 fish m^{-3}, respectively, also at least an order of magnitude higher than peak visual estimates of densities for these species. Are the orange roughy densities required to produce the observed S_v estimates credible? Based on their observations of schools of saithe (*Pollachius virens*), herring (*Clupea harengus*), and cod (*Gadus morhua*), Pitcher and Partridge (1979) concluded that an average volume per fish of 1.0 BL^3 (where BL is the fish body length) provides a reasonable approximation. For orange roughy of 34 cm *SL*, this gives an average volume per fish of 0.039 m^3 and an equivalent schooling density of 25 fish m^{-3}, suggesting that peak acoustic densities could have been orange roughy. However, considerable uncertainty remains about species composition within the high backscatter regions of the aggregation. Further work, with longer deployments and more cameras, will increase the chances of getting visual images from plume peaks to independently estimate density and species composition.

In planning for future experimental work and acoustic surveys, it would be very useful to know how plume peaks form. The most likely source of the short-term changes in acoustic backscatter is fish movement, either horizontally from elsewhere on the seamount or vertically with fish moving down from the water column or up from the seafloor. The seamount was not extensively surveyed from all orientations, so the possibility of a mobile dense aggregation of orange roughy or another species which moved around the feature cannot be ruled out. However, the area of Morgue is relatively small ($\sim$3 km^2) and dense aggregations were only detected infrequently on transects with either north–south or east–west orientation so it is not clear where the dense aggregation went to "hide" at other times. There was no evidence for aggregations intensifying due to fish moving down from the water column as acoustic densities surrounding the aggregation remained relatively constant. The most likely scenario seems to be fish movement from close to the seafloor. A proportion of fish will not be detected by acoustics because they occur close to the bottom within the acoustic dead zone (Ona and Mitson, 1996). This effect is worse in areas with steep bottom slopes. The average slope of the Morgue seamount between 900 and 1000 m depth was 16°. This is equivalent to an average dead zone height of $\sim$25 m. We know from camera observations that fish densities were higher close to the summit, and it is likely that fish moving up and down over relatively short distances from the seafloor could explain the observed variability.

Our understanding of how plume peaks form would be improved by making continuous acoustic observations from a stationary platform rather than relying on discrete transects over the aggregation. We attempted to do this from a drifting vessel, but it was impossible to remain in position with sufficient accuracy. In future work, we propose using a moored echosounder, either on the top of the mooring looking down or on the bottom of the mooring looking up, to directly monitor the temporal dynamics of the aggregation. Another advantage of using a moored echosounder is that the ranges will be much less than for a vessel-mounted echosounder. Therefore, the acoustic sampling volume will be less (more comparable with the camera sampling volume) and the acoustic dead zone will be reduced. There is also potential to use multifrequency acoustics (e.g. Kloser *et al.*, 2002) to better estimate likely species composition in plume peaks. For example, if plume peaks are formed by fast-swimming gas-bladder species then it may be possible to separate these acoustically from orange roughy.

Without further work of this type, particularly focusing on species composition on fished, as well as unfished, hills and understanding the causes for temporal variability in acoustic backscatter, acoustic estimates from surveys of deep-water seamounts (e.g. Doonan *et al.*, 2009) should continue to be treated with caution.

Acknowledgements

We gratefully acknowledge funding from the New Zealand government through Ministry of Fisheries and Land Information New Zealand Ocean Survey 2020. Particular thanks to the officers, crew, and scientific staff of RV "Tangaroa" for their expertise and dedication and for the technical assistance provided by Brett Grant and Ben Lennard. Steve Parker and two anonymous referees reviewed a draft of this paper and made many helpful suggestions and improvements.

References

Bull, B., Doonan, I., Tracey, D., and Coombs, R. 2000. An acoustic estimate of orange roughy abundance on the Northwest Hills, Chatham Rise, June–July 1999. New Zealand Fisheries Assessment Report, 2000/20. 36 pp.

Bull, B., Doonan, I., Tracey, D., and Hart, A. 2001. Diel variation in spawning orange roughy (*Hoplostethus atlanticus*, Trachichthyidae) abundance over a seamount feature on the northwest Chatham Rise. New Zealand Journal of Marine and Freshwater Research, 35: 435–444.

Clark, M. R. 2009. Deep-sea seamount fisheries: a review of global status and future prospects. Latin American Journal of Aquatic Research, 37: 501–512.

Clark, M. R., Bowden, D. A., Baird, S. J., and Stewart, R. 2010. Effects of fishing on the benthic biodiversity of seamounts of the "Graveyard" complex, northern Chatham Rise. New Zealand Aquatic Environment and Biodiversity Report, 46. 40 pp.

Clark, M. R., and O'Driscoll, R. L. 2003. Deepwater fisheries and aspects of their impact on seamount habitat in New Zealand. Journal of Northwest Atlantic Fisheries Science, 31: 441–458.

Dempster, T., and Taquet, M. 2004. Fish aggregation device (FAD) research: gaps in current knowledge and future directions for ecological studies. Reviews in Fish Biology and Fisheries, 14: 21–42.

Doonan, I., Coombs, R., and McClatchie, S. 2003. The absorption of sound in seawater in relation to estimation of deep-water fish biomass. ICES Journal of Marine Science, 60: 1047–1055.

Doonan, I. J., Dunn, M., and Hart, A. C. 2009. Abundance estimates of orange roughy on the northeastern and eastern Chatham Rise, July 2007: wide-area trawl survey and hill acoustic survey (TAN0709). New Zealand Fisheries Assessment Report, 2009/20. 41 pp.

Fofonoff, P., and Millard, R., Jr 1983. Algorithms for computation of fundamental properties of seawater. UNESCO Technical Papers in Marine Science, 44. 53 pp.

Kloser, R. J., Koslow, J. A., and Williams, A. 1996. Acoustic assessment of the biomass of a spawning aggregation of orange roughy (*Hoplostethus atlanticus*, Collett) off south-eastern Australia, 1990–93. Marine and Freshwater Research, 47: 1015–1024.

Kloser, R. J., Ryan, T., Sakov, P., Williams, A., and Koslow, J. A. 2002. Species identification in deep water using multiple acoustic frequencies. Canadian Journal of Fisheries and Aquatic Sciences, 59: 1065–1077.

Koslow, J. A., Kloser, R., and Stanley, C. A. 1995. Avoidance of a camera system by a deepwater fish, the orange roughy (*Hoplostethus atlanticus*). Deep Sea Research I, 42: 233–244.

MacLennan, D. N., Fernandes, P. G., and Dalen, J. 2002. A consistent approach to definitions and symbols in fisheries acoustics. ICES Journal of Marine Science, 59: 365–369.

McClatchie, S., and Coombs, R. F. 2005a. Low target strength fish in mixed species assemblages: the case of orange roughy. Fisheries Research, 72: 185–192.

McClatchie, S., and Coombs, R. F. 2005b. Spatial variability of orange roughy around the Northwest Hills on the Chatham Rise, New Zealand. Deep Sea Research I, 52: 589–603.

Ministry of Fisheries. 2010. Report from the Fisheries Assessment Plenary, May 2010: stock assessments and yield estimates. New Zealand Ministry of Fisheries, Wellington. 1158 pp.

O'Driscoll, R. L. 2003. Determining species composition in mixed species marks: an example from the New Zealand hoki (*Macruronus novaezelandiae*) fishery. ICES Journal of Marine Science, 60: 609–616.

O'Driscoll, R. L., and Clark, M. R. 2005. Quantifying the relative intensity of fishing on New Zealand seamounts. New Zealand Journal of Marine and Freshwater Research, 39: 839–850.

Ona, E., and Mitson, R. B. 1996. Acoustic sampling and signal processing near the seabed: the deadzone revisited. ICES Journal of Marine Science, 53: 677–690.

Pitcher, T. J., and Partridge, B. L. 1979. Fish school density and volume. Marine Biology, 54: 383–394.

Rowden, A. A., Clark, M. R., and Wright, I. C. 2005. Physical characterisation and a biologically focused classification of "seamounts" in the New Zealand region. New Zealand Journal of Marine and Freshwater Research, 39: 1039–1059.

Simmonds, E. J., and MacLennan, D. N. 2005. Fisheries Acoustics Theory and Practice, 2nd edn. Blackwell Science, Oxford. 437 pp.

Tracey, D. M., Bull, B., Clark, M. R., and Mackay, K. A. 2004. Fish species composition on seamounts and adjacent slope in New Zealand waters. New Zealand Journal of Marine and Freshwater Research, 38: 163–182.

Widder, E. A., Robison, B. H., Reisenbichler, K. R., and Haddock, S. H. D. 2005. Using red light for in situ observations of deep-sea fishes. Deep Sea Research I, 52: 2077–2085.

Wilhelmsson, D., Malm, T., and Öhman, M. C. 2006. The influence of offshore windpower on demersal fish. ICES Journal of Marine Science, 63: 775–784.

Handling editor: Bill Turrell